Antigen Presenting Cells Targeting and Stimulation Potential of Lipoteichoic Acid Functionalized Lipo-Polymerosome: A Chemo-Immunotherapeutic Approach against Intracellular Infecti...

ARTICLE *in* BIOMACROMOLECULES · FEBRUARY 2015

Impact Factor: 5.75 · DOI: 10.1021/bm5015156 · Source: PubMed

Article

pubs.acs.org/Biomac

Antigen Presenting Cells Targeting and Stimulation Potential of Lipoteichoic Acid Functionalized Lipo-Polymerosome: A Chemo-Immunotherapeutic Approach against Intracellular Infectious Disease

Pramod K. Gupta,[†] Anil K. Jaiswal,[‡] Shalini Asthana,[†] Anuradha Dube,[‡] and Prabhat R. Mishra*[,†]

[†]Pharmaceutics Division and [‡]Parasitology Division, Council of Scientific and Industrial Research-Central Drug Research Institute, B 10/1, Sector 10, Jankipuram Extension, Sitapur Road, Lucknow, India 226031

Supporting Information

ABSTRACT: Antigen presenting cells (APC) are well-recognized therapeutic targets for intracellular infectious diseases, including visceral leishmaniasis. These targets have raised concerns regarding their potential for drug delivery due to overexpression of a variety of receptors for pathogen associated molecular pathways after infection. Since, lipoteichoic acid (LTA), a surface glycolipid of Gram-positive bacteria responsible for recognition of bacteria by APC receptors that also regulate their activation for pro-inflammatory cytokine secretion, provides additive and significant protection against parasite. Here, we report the nano-architechture of APC focused LTA functionalized amphotericin B encapsulated lipo-polymerosome (LTA-AmB-L-Psome) delivery system mediated by self-assembly of synthesized glycol chitosan-stearic acid copolymer (GC-SA) and cholesterol lipid, which can activate and target the chemotherapeutic agents to *Leishmania* parasite resident APC. Greater J774A and RAW264.7 macrophage internalization of FITC tagged LTA-AmB-L-Psome compared to core AmB-L-Psome was observed by FACSCalibur cytometer assessment. This was further confirmed by higher accumulation in macrophage rich liver, lung and spleen during biodistribution study. The LTA-AmB-L-Psome overcame encapsulated drug toxicity and significantly increased parasite growth inhibition beyond commercial AmB treatment in both in vitro (macrophage-amastigote system; IC_{50}, 0.082 ± 0.009 μg/mL) and in vivo (*Leishmania donovani* infected hamsters; 89.25 ± 6.44% parasite inhibition) models. Moreover, LTA-AmB-L-Psome stimulated the production of protective cytokines like interferon-γ (IFN-γ), interleukin-12 (IL-12), tumor necrosis factor-α (TNF-α), and inducible nitric oxide synthase and nitric oxide with down-regulation of disease susceptible cytokines, like transforming growth factor-β (TGF-β), IL-10, and IL-4. These data demonstrate the potential use of LTA-functionalized lipo-polymerosome as a biocompatible lucrative nanotherapeutic platform for overcoming toxicity and improving drug efficacy along with induction of robust APC immune responses for effective therapeutics of intracellular diseases.

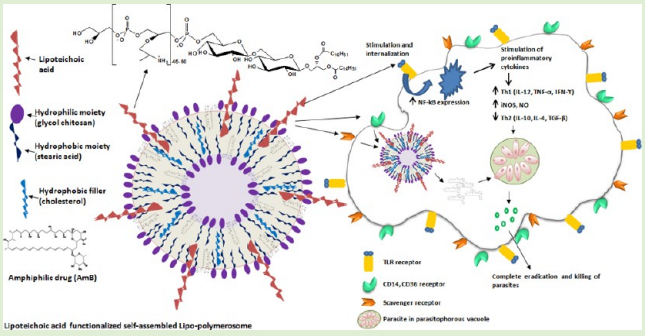

1. INTRODUCTION

The professional antigen presenting cells (APC), that is, monocytes/macrophages, B-cells, and dendritic cells, are major ports of survival of parasites into the body and play an important role in disease progression.[1] The intracellular parasite utilizes immune evasion mechanisms by down-regulation of parasite antigen presentation via the MHC class II antigen pathway and prevents activation of oxidative bursts and other microbicidal mechanisms.[2,3] These events lead to eruption of many diseases, including tuberculosis, leishmaniasis, cryptococcosis, and filariasis. Despite numerous advances over the past decades, effective intra-APC disease chemotherapy remains challenging. The generalized toxicity of many chemotherapeutic drugs makes it difficult to achieve therapeutic concentrations without systemic side effects. Consequently, architecture of such drug delivery system is essential that preferentially recognize and bind to specific overexpressed receptors on infected APC surface, with the hope that the delivery system will be internalized and release its contents specifically into the cell.[4] Such drug vehicles could potentially open the door to new therapeutic paradigms for practicing medicine that promises to eradicate a range of parasitic diseases. Additionally, the toxicity related issues of drug can be reduced by targeted delivery to intracellular regions of APC.

Taking together the immuno-stimulatory tendency of bacteria and its forced engulfment by APC, bacterial antigen can be utilized as a component of drug delivery system that will have artificial bacteria-like identity. Importantly, such delivery

Received: October 13, 2014
Revised: February 7, 2015

DOI: 10.1021/bm5015156
Biomacromolecules XXXX, XXX, XXX−XXX

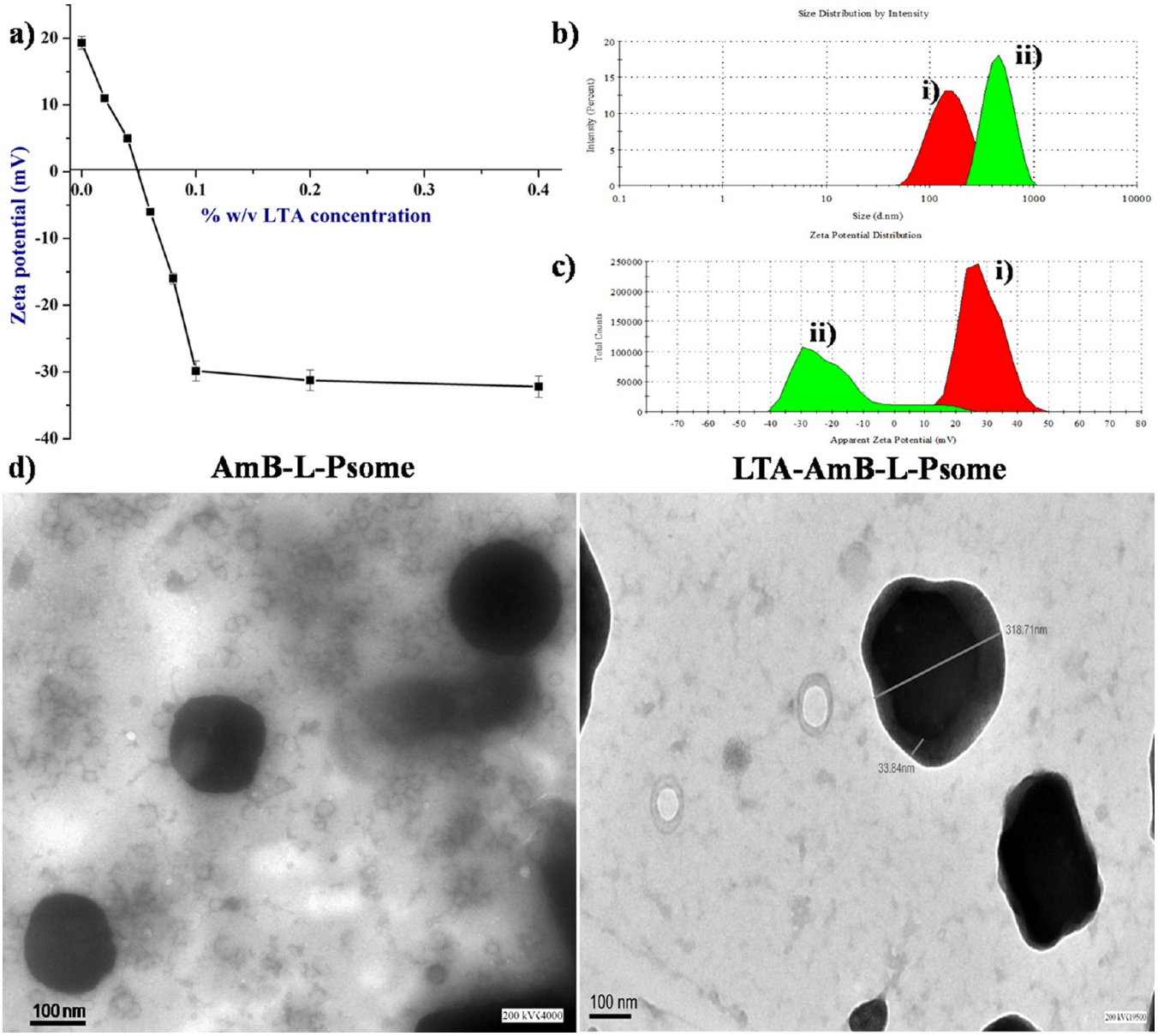

Figure 1. (a) Change in zeta potential of LTA-AmB-L-Psome during optimization of LTA concentration from 0.02 to 0.4% w/v in 10 mM HEPES buffer (pH 7.4), (b) change in size of and (c) change in zeta potential of (i) AmB-L-Psome to (ii) LTA-AmB-L-Psome, after successful absorption of LTA on the surface of AmB-L-Psome. (d) HRTEM microphotographs of AmB-L-Psome and LTA-AmB-L-Psome, while LTA functionalization was observed as a layering over AmB-L-Psome in HRTEM.

system suites as a platform for biomarker specific ligand display and affinity selection, raising the possibility that a single vehicle can be used both for identification of cell-targeting and immunostimulatory ligand for specific delivery of drug.

APC expresses a variety of receptors for pathogen associated molecular pathways (PAMPs) such as lipopolysaccharides, glycoproteins, and a range of polyanionic molecules, which get overexpressed after infection. These enable the recognition and phagocytosis of large repertoire of pathogenic parasites and subsequent generation of inflammation to eradicate the infection.

Since, lipoteichoic acid (LTA) is a common immunostimulatory polyanionic cell-wall component of *Staphylococci* and many Gram-positive bacteria, composed of poly(glycerol phosphate) attached to the glycolipid anchor β-D-Glcp^{II}-(1 → 6)-β-D-Glcp^{I}-(1 → 3)-diacylglycerol.[5,6] Because of their intra-chain phosphodiester groups, LTA collectively with teichoic acids create a negatively charged network which extends from the membrane to the surface of the bacterium and is recognized by involvement of scavenger receptor (SR) particularly type 1,[7] together with Toll-like receptors (TLRs), especially TLR2 and TLR6, and its coreceptors (CD14, CD36) of APC that results in induction of cytokines and costimulatory molecules for antigen presentation that can modulate T cell polarization. TLR specific ligands have ability to enhance drug efficacy through multiple mechanisms: TLR stimulation of APC results in increase in surface peptide/MHC complexes, costimulatory molecules, and cytokine secretion, the three signals required for T cell activation and proliferation.[8] Additionally, LTA bound to APC can interact with circulating antibodies and activate the complement cascade to induce passive immune kill phenomenon.[9] The rationale for developing this prototype formulation,

DOI: 10.1021/bm5015156
Biomacromolecules XXXX, XXX, XXX−XXX

that is, lipoteichoic acid modified lipopolymerosome (LTA-AmB-L-Psome) is to target the carrier system to antigen presenting cells (APCs) which are actually reservoir of *Leishmania* parasites and finally to impart immunostimulatory potential (being component of bacterial cell wall) to carrier system so as to evoke Th1 mediated killing of *Leishmania* parasites. This dual strategy is likely to improve pharmacokinetics and reduce toxicity to a greater extent by preventing AmB exposure to other organs.

Previously, we have reported lipo-polymerosome (L-Psome) by spontaneous self-assembly of synthesized glycol chitosan-stearic acid copolymer as stable amphotericin B (AmB) delivery system able to reduce toxicity issues.[10] In the present study, we have demonstrated better AmB chemotherapy for leishmaniasis through immuno-modulation using LTA as specific ligand anchored on lipo-polymerosome (LTA-AmB-L-Psome). Furthermore, the developed formulation has potential for its application in the condition of VL and intra-APC diseases.

2. MATERIAL AND METHODS

2.1. Materials. Glycol chitosan (GC, Mw 90 KD, 82.7% degree of deacetylation), [1-ethyl-3 (dimethylamino)propyl]carbodiimide hydrochloride (EDC), dimethylacetamide (DMAc), sodium deoxycholate (SDC), stearic acid (SA), cholesterol, fluorescein isothiocynate (FITC), Dulbecco's modified Eagle's medium (DMEM), Roswell Park Memorial Institute (RPMI) 1640 medium, streptomycin, fetal bovine serum (FBS), and LTA from *Bacillus subtilis* were purchased from Sigma-Aldrich (St. Louis, MO). Water used in all the experiments was obtained by Milli-Q Plus 185 water purification system. Methanol and acetonitrile of HPLC grade were provided by SD Fine Chem Ltd. (Mumbai, India). AmB was kindly provided as a gift sample from Emcure pharmaceutical Ltd. (Pune, India). All other reagents were of analytical grade.

Parasite and Cell Line Culture. The WHO reference strain of *L. donovani* (MHOM/IN/80/Dd8) was used for both in vitro and in vivo experiments. *Leishmania* parasites and the macrophage cell line J774A, RAW264.7 were maintained in RPMI-1640 medium (Sigma, U.S.A.) supplemented with 10% heat inactivated fetal bovine serum (HIFBS), 100 U/mL penicillin, and 100 μg/mL streptomycin at 37 °C in humidified atmosphere of 5% (v/v) CO_2/air mixture.

Animals and Ethics Statements. For in vivo antileishmanial study, Syrian golden male hamsters (*Mesocricetus auratus*, 45−50 g), for pharmacokinetic and biodistribution study, male Wistar rats (180−200 g) animal models were used while biochemical analysis and tissue histopathology performed in male Swiss mice (18−20 g) with prior approval of the Animal Ethics Committee of CSIR-Central Drug Research Institute and according to regulations of the Council for the Purpose of Control and Supervision of Experiments on Animals (CPCSEA), Ministry of Social Justice and Empowerment, Govt. of India. The Institutional Animal Ethics Committee (IAEC) Approval No. is CDRI/2012/38.

2.2. Preparation of Lipoteichoic Acid Modified Lipo-Polymerosome (LTA-AmB-L-Psome). The core self-assembled L-Psome formulation was prepared through a nanoprecipitation method followed by sonication as illustrated in our previous work.[10] For this purpose, first, we synthesized glycol chitosan-stearate copolymer through carbodiimide coupling reaction between glycol chitosan and stearic acid in molar ratio of 4:1.

Thereafter, synthesized copolymer (4 mg), AmB (1 mg in 100 μL of DMAc), and cholesterol (1 mg) was taken in 250 μL of ethanol and were mixed gently. This solution added dropwise in 1 mL of distilled water under constant stirring for 5 min in 5 mL vial. Obtained dispersion was sonicated using probe sonicator (misonix, Germany) at 20% amplitude for 120 s (15 s pulse on and 5 s pulse off), followed by dialysis against 1000 mL of water for 2 h for the purpose to remove unentrapped AmB and solvents.

In order to prepare LTA-AmB-L-Psome, the exterior surface of the L-Psome was modified using LTA ligand by adsorption method. For this purpose, 5 mg L-Psome was incubated with 1 mL LTA solution (at different concentrations from 0.02 to 0.4% w/v) in 10 mM HEPES buffer (pH 7.4) at 37 °C for 24 h to allow LTA to become electrostatically anchor onto L-Psome surface. The excess LTA was removed by washing followed by centrifugation of the resultant suspension, and the whole process was repeated thrice to ensure complete removal. The LTA amount was optimized by analyzing zeta potential change in LTA-L-Psome dispersion at 25 °C as shown in Figure 1a.

2.3. Physicochemical Characterization of L-Psome. The mean particle size, size distribution, and zeta potential of the L-Psome were determined with a Zetasizer Nano ZS (Malvern Instruments, Worcestershire, UK) at 25 °C after dilution in distilled water.

The surface morphology of optimized LTA-L-Psome was ascertained using high resolution transmission electron microscopy (HR-TEM, Tecnai G^2 F20, Eindhoven, The Netherlands).[10] To quantify LTA anchoring to L-Psome, BCA method for direct estimation of protein was performed. In this method, initially LTA decorated L-Psome eluted from sephadax G100 silica Gel column then measured by NANODROP 2000 spectrophotometer (Thermo Scientific, U.S.A.).[11−14] The coupling efficiency was expressed as the percentage of LTA bound to L-Psome surface

$$\%\text{conjugation efficiency} = \text{conjugated wt of LTA} \times 100/\text{total wt of L-Psome}$$

The solvent injection method was utilized to load the AmB within LTA-L-Psome, for this AmB solution in DMAc was added in LTA-L-Psome with constant stirring. The AmB amount encapsulated in LTA-L-Psome was quantified as the amount of unentrapped drug recovered in the supernatant by reverse phase HPLC[15] after ultracentrifugation at 40000 × g for 30 min and subsequent washings of the formulation. The percentage of drug loading, encapsulation efficiency (EE) was calculated using following formulas:

$$\text{loading efficiency} = \text{wt of (total} - \text{free) AmB in L-Psome} \times 100/\text{wt of L-Psome}$$

$$\text{encapsulation efficiency} = \text{wt of (total} - \text{free) AmB in L-Psome} \times 100/\text{wt of total AmB}$$

The release of AmB from formulations was assessed using a dialysis membrane under sink conditions. Herein, 2 mg AmB equivalent formulations (LTA-AmB-L-Psome, AmB-L-Psome, fungizone, and ambisome) was kept in dialysis bag, sealed, and placed in 200 mL of release medium with 2% w/v SDC, under continuous shaking at 100 rpm at 37 °C. A definite volume of the release medium was withdrawn at regular time intervals (30 min, and 1, 2, 3, 4, 6, 8, 12, 24, 48, 72 h) and replaced with equal volume of fresh medium. Amount of the AmB in the collected samples was analyzed using described HPLC method.

To understand stability of LTA-AmB-L-Psome, stability study was carried out at different time points (1, 7, 15, 30, 90, and 180 days) in PBS at 2−8 °C, 37 °C and room temperature along with other formulations, that is, AmB-L-Psome, ambisome, and fungizone. At each time point, an aliquot of each formulation was withdrawn for analysis to observe any change in physicochemical parameters such as size and EE of the formulation.[10]

Furthermore, rigid characteristic of LTA-AmB-L-Psome was evaluated through HRTEM study. We have observed change in surface morphology of vesicles after storage period of 6 months with 10% w/v BSA and 10% v/v Wistar rat plasma at 2−8 °C. In continuation to this, rigidity of LTA-AmB-L-Psome was also evaluated by analyzing size and PDI variation, when incubated with 10% w/v BSA and 10% v/v rat plasma at RT under gentle stirring at a concentration of 1 mg AmB/mL. At predetermined intervals up to 60 min sample was taken out and measurements were performed in triplicate.

2.4. Tagging AmB with FITC. For in vitro uptake studies, AmB was tagged with FITC as previously reported method.[11] Briefly, AmB

DOI: 10.1021/bm5015156
Biomacromolecules XXXX, XXX, XXX−XXX

(10 mg) and FITC (5 mg) were dissolved in DMAc (2 mL) followed by addition of 200 μL of triethylamine as base catalyst in 5 mL round-bottom flask, followed by 2 h stirring at room temperature and thereafter 10 mL ethyl acetate was added to precipitate the compound. Colloidal precipitate was separated by centrifugation (18000 × g for 10 min) and dried over desiccant under vacuum. In order to verify tagging of FITC with AmB (FAmB) TLC analysis was carried out using a mobile phase composed of ethyl acetate/methanol (2:3).

2.5. In Vitro Uptake by Macrophages. FAmB was encapsulated in LTA-L-Psome using same procedure as described earlier, in short, 1 mg of tagged FAmB was dissolved in 100 μL of DMAc and loaded dropwise in blank LTA-L-Psome. Infected J774A and RAW264.7 macrophage cells in 2×10^5 cells/well were placed separately on to 12-well cluster dish and cultivated in 800 μL of DMEM supplemented with 10% FBS and 1% antibiotic and antimycotic. After 24 h, the culture medium was replaced with fresh culture medium. Cells were incubated for 6 h at 37 °C and 5% CO_2 with FITC tagged formulations (LTA-FAmB-L-Psome and FAmB-L-Psome) at 10 μg/mL concentration. After incubation, cells were transferred in vials and relative fluorescence was measured by FACSCalibur (Becton Dickinson, Oxford, U.K.) at λ_{EX} (495 nm) and λ_{EM} (525 nm). FACSCalibur mediated macrophage uptake study was also carried out for noninfected as well as LTA saturated infected J774A and RAW264.7 macrophage cells.

Macrophage uptake was also assessed by confocal laser scanning microscopy (CLSM). J774A cells seeded at a density of 1×10^5 cells/well on poly-L-lysine-coated glass coverslips (in six-well plates), were left for 12 h and then incubated for 4 h with LTA-FAmB-L-Psome and FAmB-L-Psome at room temperature in the dark followed by repeated washing and fixed in 10% formalin in PBS and observed by CLSM (Carl Zeiss LSM5100, Germany) equipped with ×40 objective lens. λ_{EX} (495 nm) and λ_{EM} (525 nm) of FITC were used to analyze tagged AmB.

2.6. Pharmacokinetic and Biodistribution Study. Wistar rats (180−200 g) were allocated into the following four treatment groups: IV bolus administration of 5 mg/kg AmB-L-Psome (n = 6), 5 mg/kg LTA-AmB-L-Psome (n = 6), 1 mg/kg fungizone (n = 6), and 5 mg/kg ambisome (n = 6). The doses selected for IV administration of commercial AmB formulations in the present study are in the range for which there is no clinical nephrotoxicity for each formulation, based on published reports.[16] Systemic blood (0.25 mL) was sampled at 10 min predose and 0.5, 1, 2, 3, 5, 8, 12, 24, 48, and 72 h postdose of IV bolus administrations of AmB formulations, followed by separation of plasma by centrifugation at 2500 × g for 10 min at 15 °C). The animals were sacrificed at 0.5, 1, 2, 3, 5, 8, 12, 24, 48, and 72 h post administration of AmB formulations, and liver, spleen, right lung, right kidney, and heart were harvested for drug analysis. Plasma and tissue samples were stored at −80 °C until drug analysis.

Samples were analyzed using Shimadzu HPLC system equipped with 10 ATVP binary gradient pumps (Shimadzu, Japan), a Rheodyne model 7125 injector (CA, U.S.A.) with a 20 μL loop and SPD-M10 AVP UV detector (Shimadzu, Japan). AmB in plasma and tissue samples was analyzed following published validated isocratic HPLC method with slight modifications,[15] using column [LichroCART 250−4, Lichrospher 100, RP-18e, 5 μm, 250 × 4 mm (Merck KgaA, 64271 Darmstadt, Germany)] and mobile phase [acetonitrile/10 mM KH_2PO_4 buffer, pH 4 (60:40, v/v)] at a flow rate of 1 mL/min. Tissue samples were homogenized in acetonitrile (1 g tissue per 2 mL acetonitrile) using IKA T25 digital ULTRA-TURRAX for 3−4 min over an ice bath. The filtered aliquots of 20 μL of processed plasma and tissues were used for quantitative analysis. Calibration curves of AmB were linear in the range of 0−10 μg/mL for plasma and 0−10 μg/g for tissue samples. The AmB quantification limit for plasma was 20 ng/mL and for tissue samples was 20 ng/g.

2.7. In Vitro Antiamastigote Activity. The activity of AmB-formulations against intracellular amastigotes was evaluated as per protocol described earlier.[17] Briefly, J774A macrophages (1×10^5 cells/well) in 24-well plates were infected with green fluorescent protein (GFP) expressed promastigotes at multiplicity of 10 parasites per macrophage. After 12 h incubation 24-well plates were washed thrice with PBS (pH 7.4) to remove nonphagocytosed promastigotes and resupplemented with RPMI-1640 complete medium, followed by incubation with LTA-AmB-L-Psome, AmB-L-Psome, ambisome, and fungizone at different drug concentrations, and with the same amount of blank formulations in triplicate. After 48 h incubation, cells were removed, washed in PBS and quantitated by FACSCalibur cytometer equipped with a 20 mW argon laser at 488 nm excitation and 515 nm emission followed by data analysis using Kaluza analysis software (Beckman Coulter). The parasite growth inhibition was determined by relative fluorescence levels of drug-treated parasites with that of untreated control parasites and the inhibitory concentrations (IC_{50} and IC_{90}) were calculated using GraphPad Prism6.

2.8. In Vivo Assay in *L. donovani* Infected Hamsters. The in vivo AmB-formulation efficacy was studied against *L. donovani* amastigotes in a golden hamster model.[10] After 30 days of established infection, hamsters (n = 5 in each group) were intraperitoneally dosed 1 mg/kg of LTA-AmB-L-Psome, AmB-L-Psome, fungizone, and ambisome each for five consecutive days. Two-week, post-treatment, treated animals were sacrificed and results were compared with the infected untreated control group. Detection of parasitic load in spleen was carried out by blinded microscopic enumeration with Giemsa-stained spleen impression smear. Parasite burdens were calculated by counting the number of amastigotes per 100 macrophage nuclei. The percentage of inhibition (PI) was calculated using the formula:

$$PI = (PP - PT/PP) \times 100$$

where PP and PT are number of amastigotes per 100 macrophage nuclei before and after treatment, respectively.

2.9. Nitric Oxide (NO) Determination. NO content in the splenocytes culture supernatants of treated hamsters was monitored by Griess assay method.[18] Briefly, the culture supernatant and the mixture of Greiss reagent [1% sulfanilamide 1 N HCl and 0.1% N-(1-naphthyl) ethylenediamine dihydrochloride in H_2O] were mixed at 1:1 ratio and incubated for 15 min at room temperature, and the absorbance was determined at 540 nm by microplate reader (DTX 800 multimode detector, Beckman Coulter). Nitrite concentration was calculated with a sodium nitrite standard curve generated for each experiment.

2.10. Evaluation of Th1/Th2 Cytokines and Chemokine. Splenic cell smear of treated and untreated control groups were analyzed for various cytokines (TNF-α, IL-12, IFN-γ, IL-4, IL-10, and TGF-β) and inducible nitric oxide synthase (iNOS) using quantitative real time-PCR (qRT-PCR) technique. Splenocytes mRNA of different hamster groups was isolated using Tri reagent (Invitrogen, U.S.A.) followed by cDNA synthesis using first strand cDNA synthesis kit (Fermentas, U.S.A.) as per manufacturer's protocol. qRT-PCR was conducted with initial denaturation at 95 °C for 2 min followed by 40 cycles, each consisting of denaturation at 95 °C for 30s, annealing at 55 °C for 40 s, and extension at 72 °C for 40 s per cycle using the iQ5 multicolor real-time PCR system (Bio-Rad, U.S.A.). Comparator samples were cDNAs from infected hamsters. The PCR signals quantification was performed by comparing the cycle threshold (CT) value of the gene of interest with that of reference gene hypoxanthine phosphoribosyltransferase (HPRT). Results were expressed as fold change (FC) of mRNA relative to those in unstimulated cells.

2.11. Toxicity Assay. The hemolysis and J774A cell cytotoxicity assay was performed in 5 to 20 μg/mL AmB concentrations of LTA-AmB-L-Psome, AmB-L-Psome, and their equivalent blank formulations using methods reported previously.[15] Subacute toxicity assay was performed in five mice groups (n = 3), received LTA-AmB-L-Psome (5 mg/kg), AmB-L-Psome (5 mg/kg), ambisome (5 mg/kg), fungizone (1 mg/kg), and saline (control group) intravenously in a constant volume of 200 μL daily for 15 days. A total of 12 hours post-treatment, animals were euthanized, and blood was collected by cardiac puncture, centrifuged (2000 × g), and subsequently analyzed for biochemical parameters. Transaminase activities, urea and creatinine were determined using an automatic Hitachi 912 apparatus (Roche Diagnostics Corporation, Indianapolis, IN, U.S.A.). Kidney, liver, spleen, lung, heart, and colon tissues were collected for histopathological studies, as reported in our previous publication.[10]

DOI: 10.1021/bm5015156
Biomacromolecules XXXX, XXX, XXX−XXX

Table 1. Characterization of AmB Formulations[a]

name of formulation	particle size (nm)	polydispersity index (PDI)	zeta potential (mV)	drug loading (% w/w)	encapsulation efficiency	LTA bound (% w/w)
AmB-L-Psome	341.1 ± 12.3	0.197 ± 0.02	(+)19.32 ± 0.85	25.59 ± 0.87	89.58 ± 1.25	
LTA-AmB-L-Psome	443.1 ± 17.6	0.196 ± 0.11	(−)29.84 ± 0.51	25.26 ± 0.65	89.76 ± 1.41	6.29 ± 0.34

[a]All data are represents as average of $n = 3$.

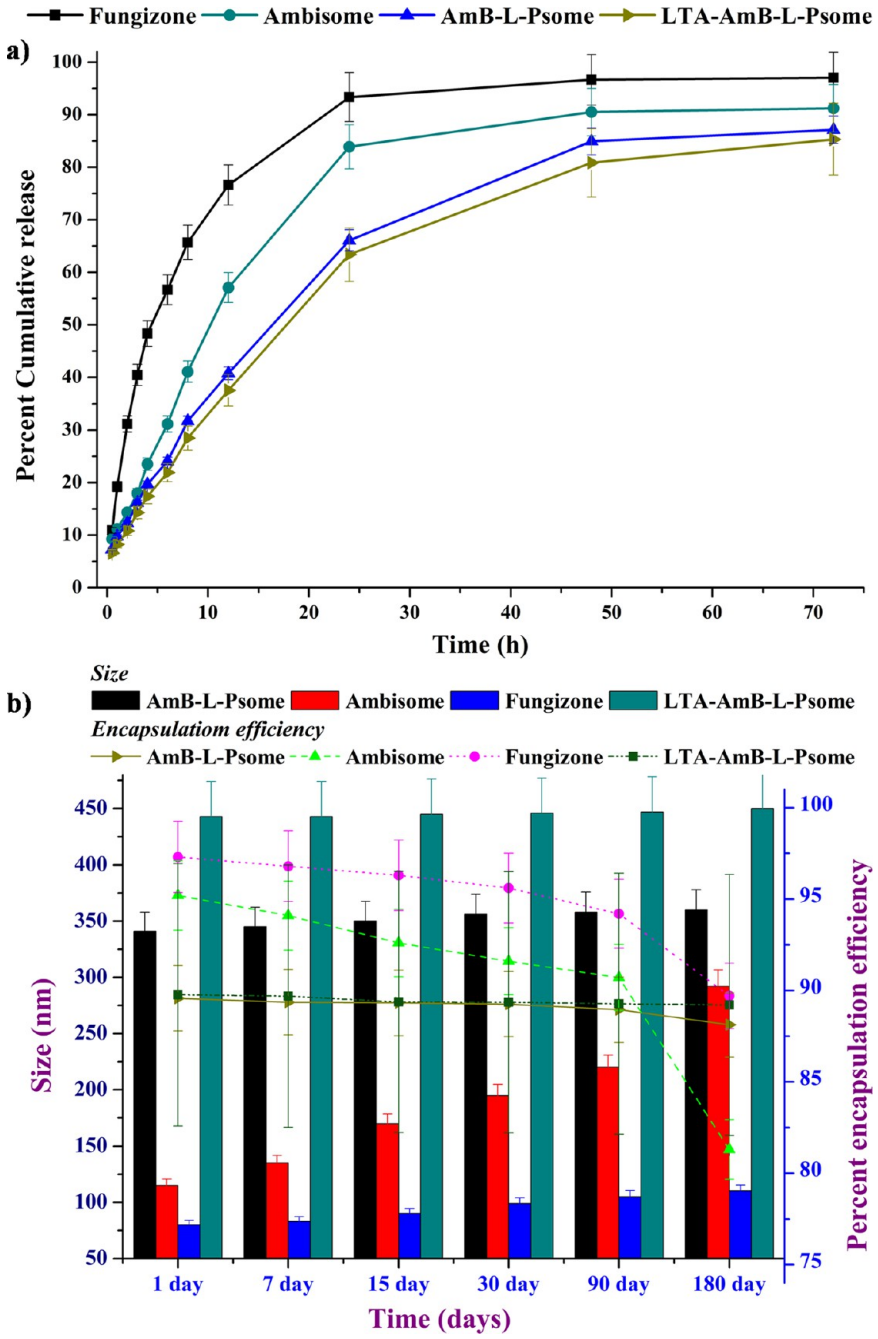

Figure 2. (a) In vitro drug release study of different AmB formulations (LTA-AmB-L-Psome, AmB-L-Psome, ambisome, and fungizone) in PBS with 2% w/v sodium deoxycholate (SDC), pH 7.4 at different time intervals. (b) Stability study of LTA-AmB-L-Psome, AmB-L-Psome, ambisome, and fungizone after incubation for different time at 2−8 °C in PBS. The changes in size and encapsulation efficiency of different formulations were measured over a period of time during stability study.

2.12. Statistical Analysis. All results are presented as mean ± standard deviation (S.D.) of three independent measurements. Data were analyzed by one-way analysis of variance (ANOVA) and p value of <0.05 was considered significant in all cases.

3. RESULTS

3.1. Preparation and Characterization of LTA-L-Psome. In the present study, glycol chitosan (GC) component of synthesized amphiphilic copolymer act as hydrophilic shell

DOI: 10.1021/bm5015156
Biomacromolecules XXXX, XXX, XXX−XXX

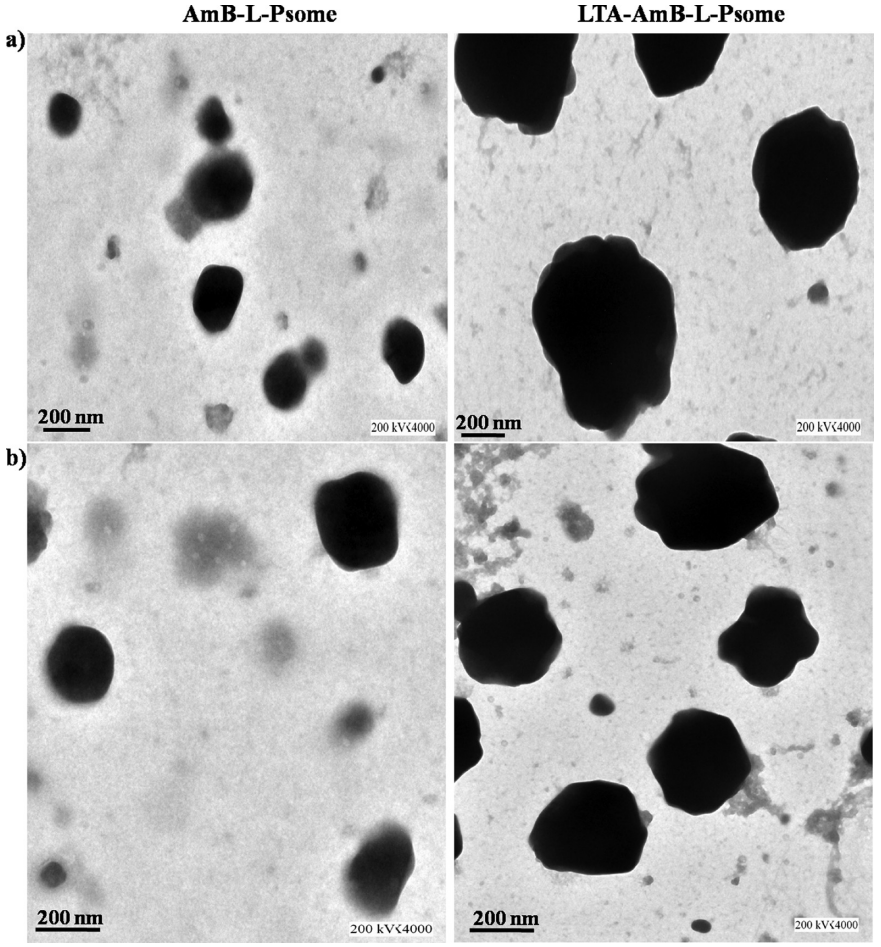

Figure 3. HRTEM images of AmB-L-Psome and LTA-AmB-L-Psome showing morphology (size and shape) after 6 month storage in (a) 10% w/v BSA and (b) 10% v/v rat plasma.

and stearic acid (SA) served as hydrophobic core and cholesterol as model lipid to form lipid monolayer at the interface of GC shell and SA core. The GC-SA copolymer self-assembled along with lipid and form AmB-L-Psome are more stable than native lipid structure since it has properties of both liposome and nanoparticles. Further, high energy sonication method was used to prepare AmB-L-Psome, which has positive surface charge of (+) 19.32 ± 0.85 mV and size of 341.1 ± 12.3 nm [polydispersity index (PDI) 0.197 ± 0.02, as shown in Figure 1b,c]. The electrostatic adsorption method was utilized for construction of LTA-AmB-L-Psome from AmB-L-Psome. The AmB-L-Psome was surface decorated with LTA by means of electrostatic interaction between positively charged AmB-L-Psome and negatively charged LTA leads to formation of LTA-AmB-L-Psome with zeta potential (−) 29.84 ± 0.51 mV and particle size 443.1 ± 17.6 nm (PDI 0.196 ± 0.11) at optimized 0.1% w/v concentration of LTA (Figure 1a−c). The charge reversal from positive to negative confirms successful formation of LTA-AmB-L-Psome. Figure 1d shows the morphological characteristics of the LTA-AmB-L-Psome by HRTEM. The HRTEM shows almost spherical morphology of LTA-AmB-L-Psome. The LTA layer of ∼34 nm over L-Psome was observed in HRTEM further confirmed decoration of LTA on the surface of L-Psome. Entrapment efficiency (EE) and drug loading in LTA-AmB-L-Psome was found to be 89.76 ± 1.41 and 25.26 ± 0.65%, respectively (Table 1). The LTA-AmB-L-Psome releases 63.37 ± 5.32%w/w AmB in 24 h that found to be sustained among other formulations as shown in Figure 2a. LTA-AmB-L-Psome, AmB-L-Psome, and fungizone did not show significant changes in size and EE, while ambisome presented drastic changes in size and EE during storage at 2−8 °C (Figure 2b), as well as at 37 °C and room temperature (Supporting Information, Figure S1).

In context to rigidity evaluation of LTA-AmB-L-Psome, HRTEM images did not show any major/identifiable changes in shape of vesicles, after six month storage along with 10% w/v BSA (Figure 3a) and 10% v/v rat plasma (Figure 3b). Furthermore, LTA-AmB-L-Psome has shown negligible increase in size and PDI, while slight increase in size was observed in case of AmB-L-Psome and fungizone. In contrast, ambisome had a dramatic increase in size and PDI within 20 min of incubation in BSA as well as in rat plasma (Supporting Information, Figure S2).

3.2. In Vitro Macrophage Uptake of LTA-FAmB-L-Psome. FITC dye was tagged to AmB (FAmB) in order to provide fluorescence and characterized using TLC where RF value of FAmB was slightly higher than AmB and far less than FITC.

The in vitro uptake of LTA-FAmB-L-Psome was ∼2.5-fold and ∼3.7-fold higher compared to FAmB-L-Psome by infected J774A (Figure 4i) and RAW264.7 (Figure 4ii) macrophage cells, respectively, in relative concentration. Data of cellular uptake by noninfected as well as LTA saturated infected J774A and RAW264.7 macrophage are presented in Supporting

DOI: 10.1021/bm5015156
Biomacromolecules XXXX, XXX, XXX−XXX

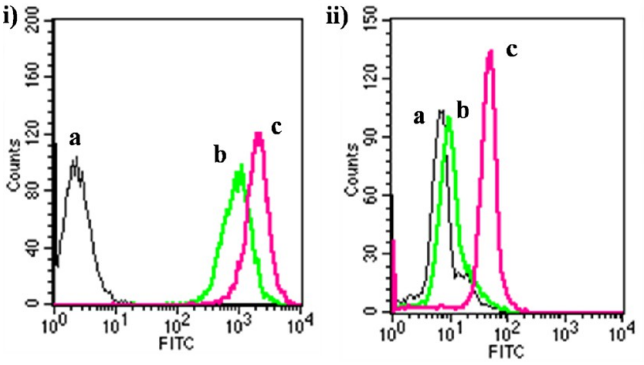

Figure 4. In vitro uptake study of (a) control, (b) FAmB-L-Psome, and (c) LTA-FAmB-L-Psome by infected (i) J774A and (ii) RAW264.7 macrophage cell line after 6 h incubation.

Information, Figure S3i,ii. Furthermore, the confocal microscopic image demonstrates the localization and distribution of tagged LTA-FAmB-L-Psome in J774A macrophage cells. The most of LTA-FAmB-L-Psomes were internalized within cells, located and distributed in complete cells, although relatively reduced amount of FAmB-L-Psome was internalized in cells, showing green fluorescence arising from FITC tagged AmB (Figure 5).

3.3. Pharmacokinetics and Tissue Distribution of Different AmB-Formulations. Macrophage targeting potential of LTA-AmB-L-Psome was evaluated in vivo by studying AmB tissue distribution and pharmacokinetics in rats following IV bolus administration of test and commercially available formulations. Figure 6 and Table 2, shows pronounced differences in plasma concentration−time profiles and the calculated pharmacokinetic parameters. LTA-AmB-L-Psome and AmB-L-Psome showed lower plasma drug concentrations than ambisome due to slower release rate as a result of the higher rigidness and molecular interaction with GC-SA copolymer.[10] Lower AmB clearance was observed in case of LTA-AmB-L-Psome compared to fungizone. LTA-AmB-L-Psome showed significantly higher AmB distribution at all time points in spleen, liver, and lung while very fewer disposition in kidney compared with AmB-L-Psome, ambisome, and fungizone. Furthermore, accumulated amounts of AmB in heart were found to be almost negligible for the tested formulations.

3.4. Inhibitory Effect on *L. donovani* Intramacrophage Amastigotes and In Vivo Antileishmanial Activity. Results are expressed in terms of dose response curve and inhibitory concentration (IC_{50}, IC_{90}; Figure 7a,b). Formulation LTA-AmB-L-Psome (IC_{50}, 0.082 ± 0.009 μg/mL) showed significant improvement in efficacy as compared to AmB-L-Psome (IC_{50}, 0.14 ± 0.021 μg/mL) and commercial formulations [fungizone (IC_{50}, 0.295 ± 0.076 μg/mL) and ambisome (IC_{50}, 0.192 ± 0.046 μg/mL)]. The in vivo experimental data as shown in Figure 7c clearly revealed that LTA-AmB-L-Psome was significantly more active (89.25 ± 6.44% inhibition) compared to AmB-L-Psome (66.46 ± 2.65% inhibition; $p < 0.01$), ambisome (62.37 ± 3.13% inhibition; $p < 0.05$), and fungizone (56.54 ± 3.91% inhibition; $p < 0.05$), while drug-free LTA-L-Psome and L-Psome showed 11.72 ± 0.65% and 4.35 ± 0.61% parasite growth inhibition, respectively.

3.5. Measurement of NO. NO is one of the most potent APC-derived versatile microbicidal player in the immune system, involved in the pathogenesis and control of various infectious diseases.[19] We therefore investigated the generation of NO in culture supernatants of splenocytes isolated from the

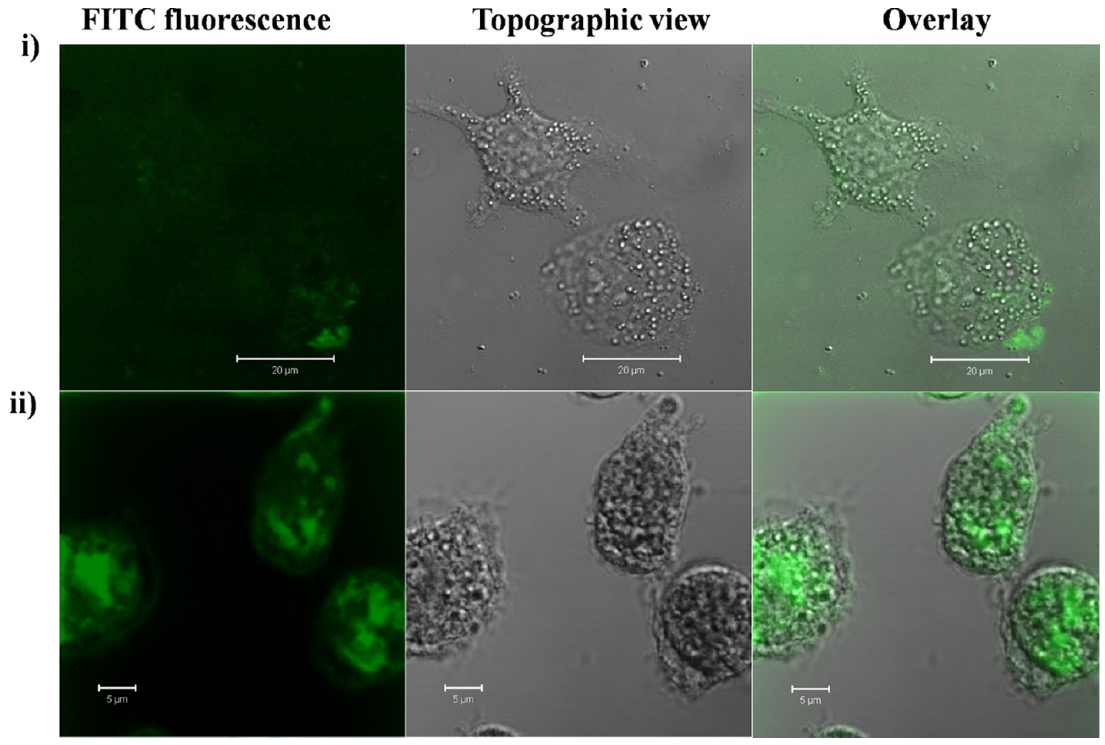

Figure 5. CLSM image of adherent cell cultures treated with (i) FAmB-L-Psome and (ii) LTA-FAmB-L-Psome. There is complete internalization of LTA-FAmB-L-Psome seen as green fluorescence in infected J774A macrophage cells.

DOI: 10.1021/bm5015156
Biomacromolecules XXXX, XXX, XXX−XXX

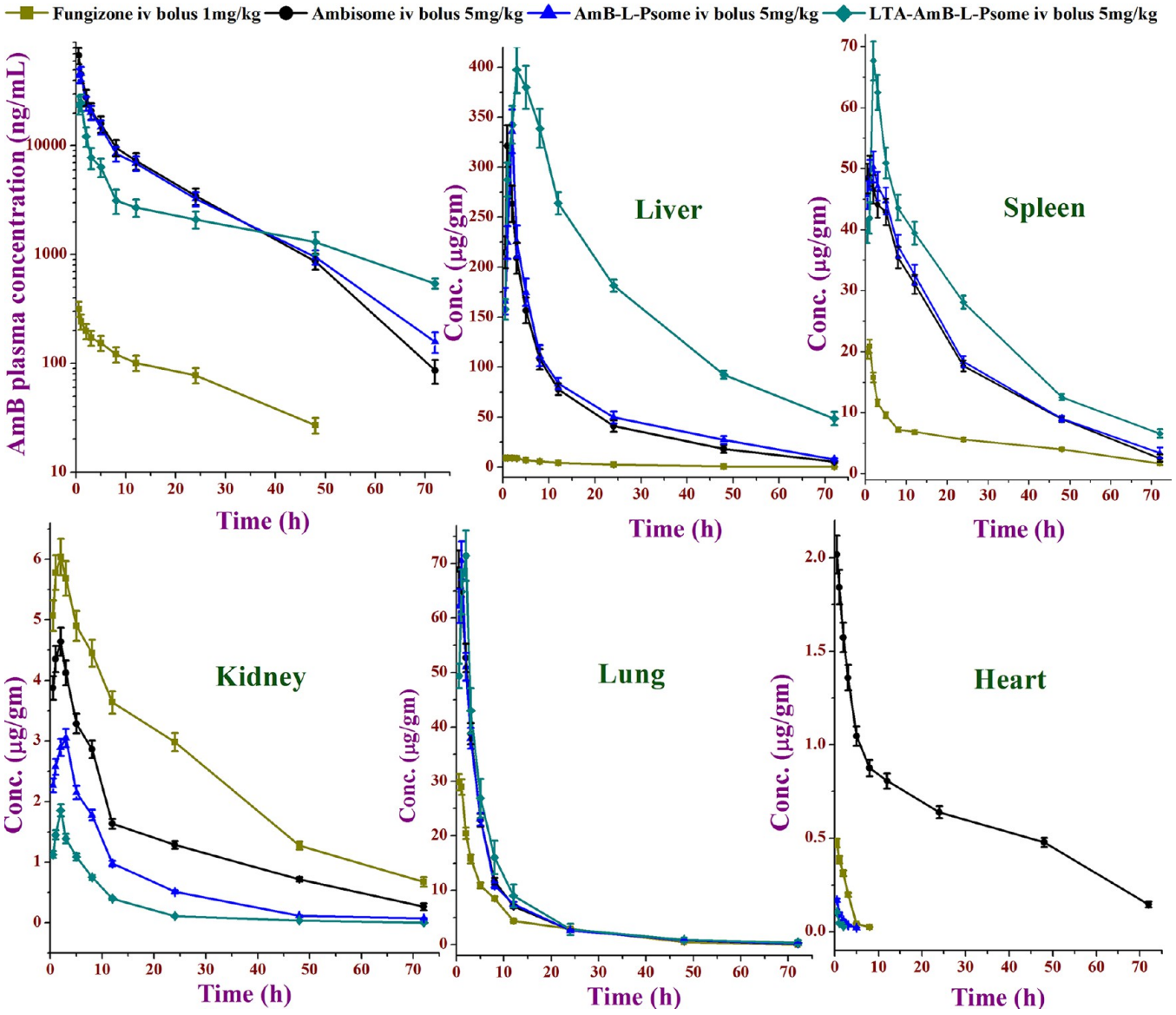

Figure 6. Plasma AmB concentration−time semilogarithmic plot (mean ± SEM), liver, spleen, lung, kidney, and heart AmB concentration−time plot (mean ± SEM), following iv bolus administration of fungizone 1 mg/kg, ambisome 5 mg/kg, AmB-L-Psome 5 mg/kg, and LTA-AmB-L-Psome 5 mg/kg. (n = 3).

Table 2. Pharmacokinetic Parameters of AmB Formlations[a]

AmB equivalent concentration in formulation	fungizone 1 mg/kg	ambisome 5 mg/kg	AmB-L-Psome 5 mg/kg	LTA-AmB-L-Psome 5 mg/kg
AUC_{0-72} (h × ng/mL)	4464.4 ± 526.3	342739.3 ± 28461.5	317360.3 ± 48697	188640.2 ± 3978.5
$t_{1/2}$ (h)	17.7 ± 2.6	11.8 ± 1.9	12.6 ± 3.4	47.9 ± 8.4
CL (mL/h/kg)	207.0 ± 21.8	14.5 ± 1.6	15.6 ± 2.5	23.7 ± 4.3
MRT_{0-72} (h)	15.9 ± 4.1	11.5 ± 2.8	12.9 ± 3.1	30.0 ± 6.8

[a]Each data represents the mean ± standard deviation (n = 3).

different experimental groups as mentioned above. A significant increase in nitrite generation was detected in LTA-AmB-L-Psome-treated hamster (Figure 8i(a)).

3.6. Cytokine Assay. The relative fold change of Th1 and Th2 cytokine expression levels was evaluated by qRT-PCR with different formulations, that is, LTA-AmB-L-Psome, AmB-L-Psome, and blank LTA-L-Psome having AmB concentration equivalent to commercial formulations fungizone and ambisome, as shown in Figure 8ii. The iNOS expression was found to be significantly up-regulated (p < 0.05) in LTA-AmB-L-Psome and LTA-L- Psome (Figure 8i(b)). The Th1 cytokine expression of TNF-α, IFN-γ, and IL-12 was significantly elevated (p < 0.01) in all treated groups in comparison with that of the *L. donovani* infected group but it is higher in LTA-AmB-L-Psome (p < 0.05) compared to all other formulations (Figure 8ii(a)). In contrast, the expression of TGF-β, IL-10, and IL-4 was found to be down-regulated (p < 0.05) significantly in the hamsters in all treated groups but their levels were minimum with LTA-AmB-L-Psome among other formulations as shown in Figure 8ii(b).

DOI: 10.1021/bm5015156
Biomacromolecules XXXX, XXX, XXX−XXX

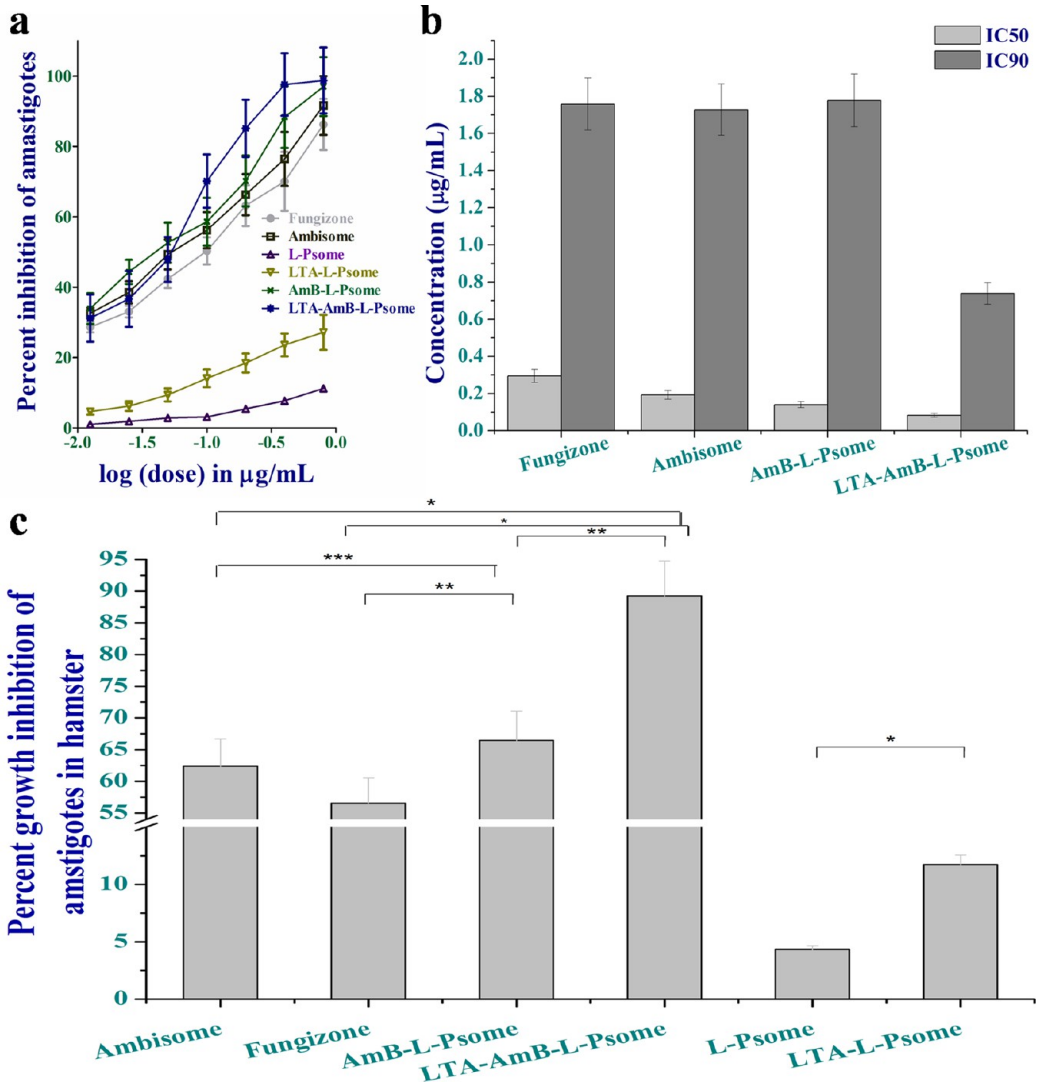

Figure 7. (a) In vitro dose−response curve of LTA-AmB-L-Psome, AmB-L-Psome, ambisome, fungizone, LTA-L-Psome, and L-Psome with the different concentration of formulations against *L. donovani* amastigote infected macrophages observed after 48 h of incubation (n = 3). (b) In vitro antileishmanial activity (IC_{50} and IC_{90}) of LTA-AmB-L-Psome, AmB-L-Psome, fungizone, and ambisome in *L. donovani* amastigote infected macrophages observed after 48 h of incubation (n = 3). (c) In vivo antileishmanial activity of LTA-AmB-L-Psome, AmB-L-Psome, fungizone, and ambisome in the established Syrian golden hamster model infected with *L. donovani* amastigotes at an intraperitoneal dose of 1 mg of AmB/kg body weight of hamster and formulations without drug were injected intraperitoneally into each hamster on day 31 postinfection. The parasite burden was estimated by splenic biopsy on day 15 post-treatment and percentage parasite inhibition was calculated in comparison with the parasite burden of untreated infected animals (means ± SD; n = 5). The mean parasite burden in the spleen of untreated, infected control animals was 454 ± 38 amastigotes per 100 cell nuclei of macrophages. (n = 5). *p < 0.05 for LTA-AmB-L-Psome vs ambisome, LTA-AmB-L-Psome vs fungizone, and Lec-L-Psome vs L-Psome; **p < 0.01 for LTA-AmB-L-Psome vs AmB-L-Psome, AmB-L-Psome vs fungizone; ***p < 0.001 for AmB-L-Psome vs ambisome.

3.7. Toxicity Assay of the Formulations. Developed LTA-AmB-L-Psome and LTA-L-Psome exhibited hemotoxicity up to 7.43 ± 0.52% and 0.98 ± 0.16%, as shown in Figure 9a. The cytotoxicity (reversal of % cell viability) induced by various concentrations of LTA-AmB-L-Psome was less than 6%, as shown in Figure 9b. The levels of serum aspartate aminotransferase (ASAT) and alanine aminotransferase (ALAT) was found to be significantly elevated in case of fungizone and ambisome, while it is lower in LTA-AmB-L-Psome and AmB-L-Psome as shown in Figure 9c. The level of serum creatinine and blood urea increased significantly (>3 fold; p < 0.05) in mice treated with fungizone, while these levels in case of ambisome, LTA-L-Psome, and LTA-AmB-L-Psome were similar, as shown in Figure 9c. The histopathology of kidney tissue revealed patchy tubules, redness, and necrosis in fungizone-treated mice, as shown in Figure 10, while other formulations showed normal pattern in histopathology of kidney tissues. Further, fungizone showed very slight redness in spleen tissues (Figure 10). Normal histopathology was observed in ambisome-treated mice except minute redness in liver tissues, as depicted in Figure 10. However, LTA-AmB-L-Psome and AmB-L-Psome shows normal histopathology in all tissues.

4. DISCUSSION

Efficient and cost-effective treatment of leishmaniasis remains a challenge and reckoned as high priority area of research in developing countries. AmB is currently the second line drug of choice for leishmaniasis therapeutics with 97% cure rate and no

DOI: 10.1021/bm5015156
Biomacromolecules XXXX, XXX, XXX−XXX

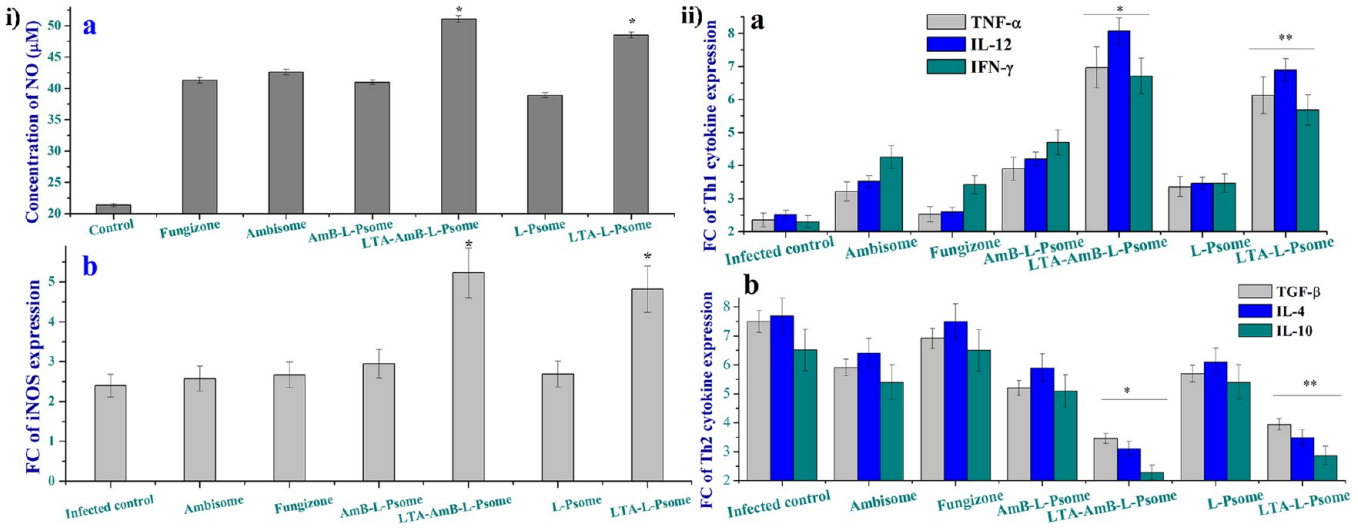

Figure 8. (i) (a) Concentration of NO, (b) relative fold change of iNOS expression; (ii) (a) relative fold change of Th1 cytokines expression and (b) relative fold change of Th2 cytokine expression, in splenocytes of infected hamsters after treatment of equivalent amount of 1 mg AmB/kg of fungizone, ambisome, LTA-AmB-LPsome, AmB-L-Psome, and, similar amount of LTA-L-Psome, L-Psome without drug and control.

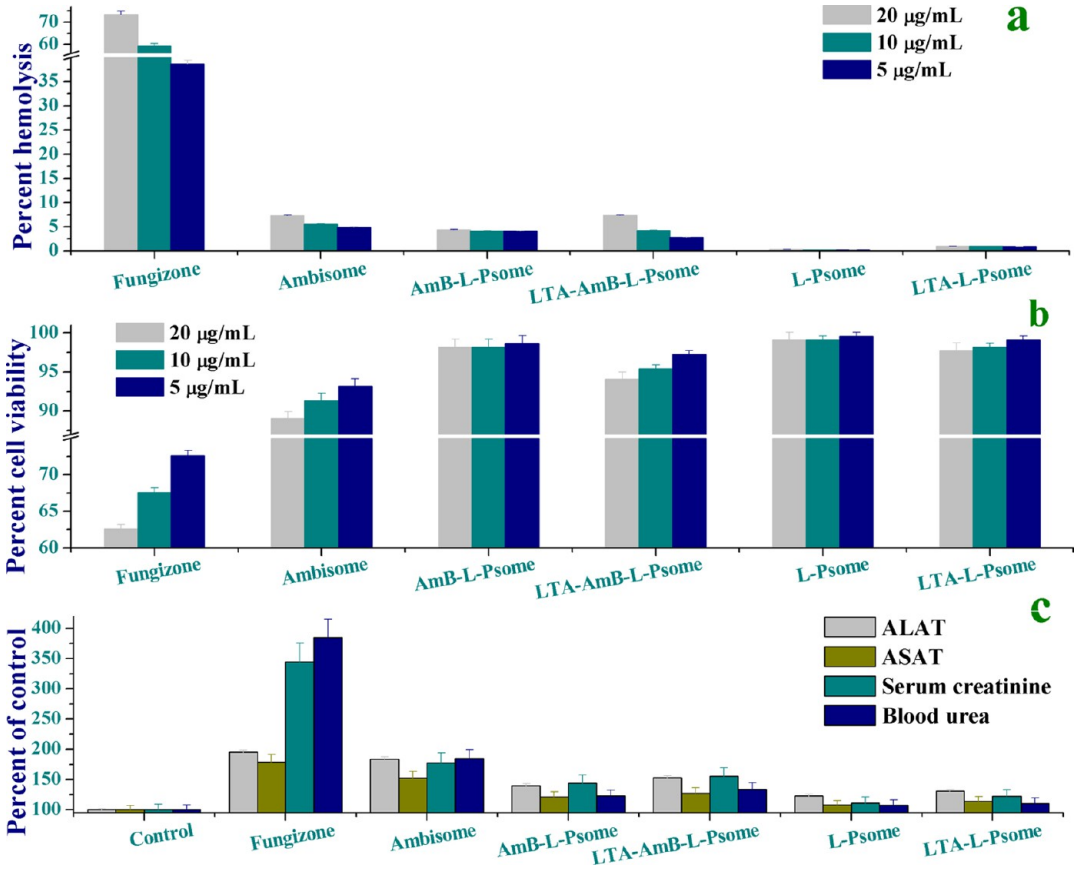

Figure 9. Effect of fungizone, ambisome, AmB-L-psome, LTA-AmB-L-Psome, LTA-L-Psome, and L-Psome equivalent to amphotericin B concentration of 5, 10, and 20 μg/mL on (a) RBCs collected from Wistar rat's blood and (b) J774A macrophage cell line (n = 3). (c) Serum biochemical analysis of transaminases: aspartate aminotransferase (ASAT), alanine aminotransferase (ALAT), serum creatinine, and blood urea of mice received saline (control group), fungizone (1 mg/kg), ambisome (5 mg/kg), LTA-AmB-L-Psome (5 mg/kg), AmB-L-Psome (5 mg/kg), LTA-L-Psome, and L-Psome intravenously in a constant volume of 200 μL daily for 15 days (n = 3).

reported resistance.[20] The use of AmB is limited by dose-dependent toxicities, especially the nephrotoxicity.[21] Therefore, the present study focuses on the development of the AmB encapsulated LTA decorated lipo-polymerosome (LTA-AmB-L-Psome), which can efficiently provide parasite resident APC specific targeted delivery of AmB, able to eliminate undesirable toxic side effects and at the same time it modulates immune response to completely eradicate parasites from host cells.

The present study describes a novel targeting and immunomodulatory approach for antileishmanial therapy. By

DOI: 10.1021/bm5015156
Biomacromolecules XXXX, XXX, XXX−XXX

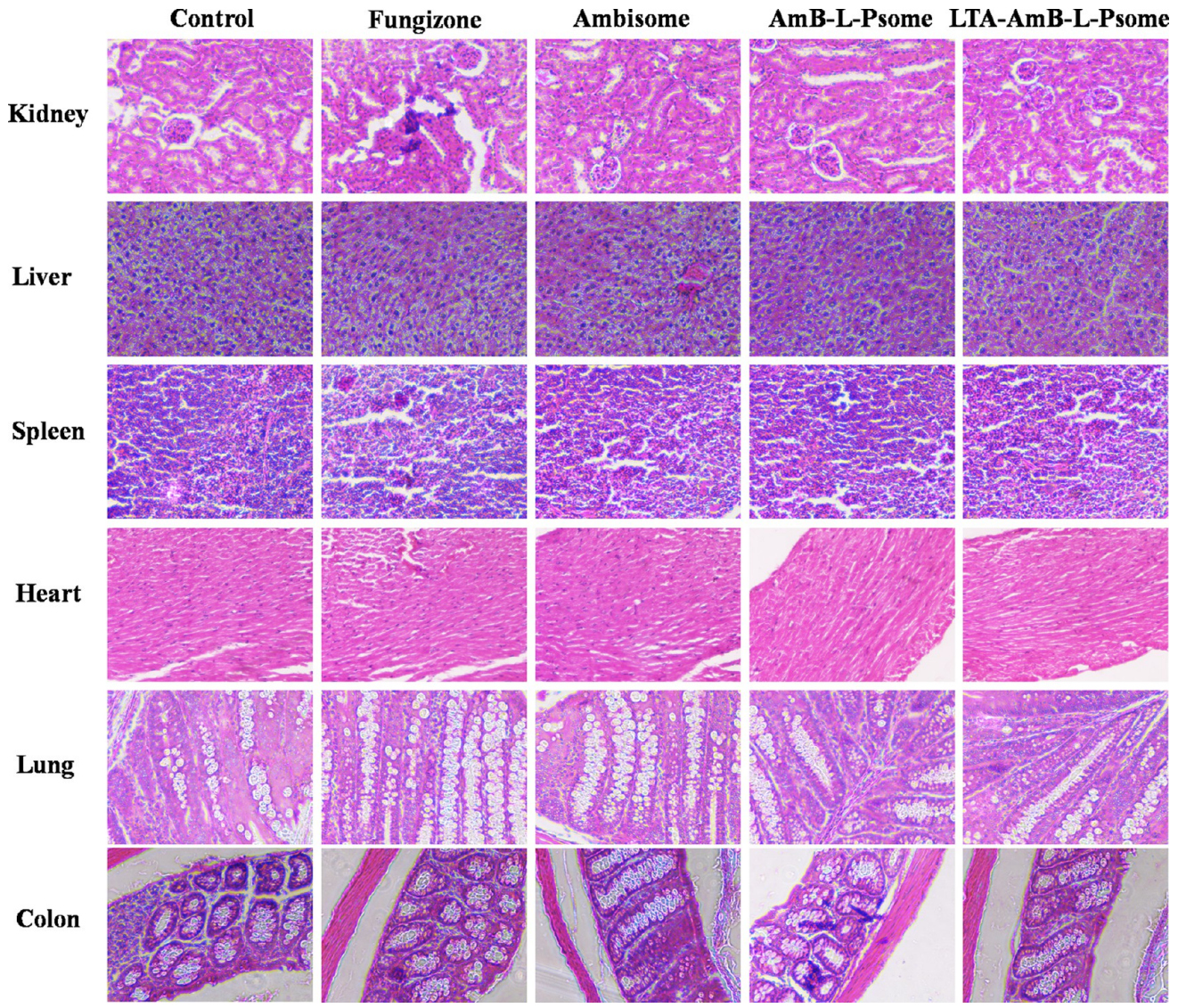

Figure 10. Histopatology of kidney, liver, spleen, lung, heart and colon tissues after treatment of mice with saline (control group), fungizone (1 mg/kg), ambisome (5 mg/kg), AmB-L-Psome (5 mg/kg), and LTA-AmB-L-Psome (5 mg/kg) intravenously in a constant volume of 200 μL daily for 15 days (n = 3).

employing the LTA-L-Psome as AmB delivery system, antileishmanial efficiency is significantly increased both in vivo and in vitro. This, together with low toxicity of LTA-AmB-L-Psome due to specific targeting and preferential uptake by infected macrophages, provide an opportunity for this system to be a viable carrier for further drug development. Components used for LTA-L-Psome formulation, make it more economical than existing liposomal AmB.

Interestingly, LTA-L-Psome provide sandwiched properties both polymeric nanoparticles and liposomes, while excluding some of their limitations such as drug payload, stability, controlled, and targeted release at site of infection, solubility, and pharmacokinetic profile. The use of biocompatible GC and SA polymers has advantage over other formulations in terms of ease of preparation, longer shelf life and better stability in biological fluids with absence of side effects.[10] For fabrication, we dissolved synthesized copolymer GC-SA in DMAc and cholesterol in ethanol, where they get self-assembled in order to reduce free energy at the concentric interfaces of water. Subsequently, self-assembled structures are dispersed in water phase through vigorous vortexing followed by solvent evaporation and sonication. The AmB-L-Psome surface with positive potential [(+)19.32 ± 0.85] can easily be functionalized with lipoteichoic acid targeting ligand. The LTA was decorated on L-Psome surface using electrostatic adsorption method where LTA binds through polyanionic hydrophilic chains via strong electrostatic interaction on cationic L-Psome surface. LTA creates a negatively charged network because of the interchain phosphodiester groups,[6,22] results in development of anionic LTA-AmB-L-Psome [(−)29.84 ± 0.51].

The HR-TEM image of LTA-AmB-L-Psome (Figure 1d) was found to be nearly spherical and an opaque layer on L-Psome depicted LTA adsorption on L-Psome. Increase in size and reversal in zeta potential from positive to negative also suggest adsorption of LTA on L-Psome as observed in Figure 1b,c. The adsorption efficiency of LTA on L-Psome surface was calculated and adsorption was confirmed by BCA protein assay method (Table 1). The LTA-AmB-L-Psome has ability to release AmB in sustained rate than other formulations, due to additional LTA coating on AmB-L-Psome surface.[10,15] LTA-

DOI: 10.1021/bm5015156
Biomacromolecules XXXX, XXX, XXX−XXX

AmB-L-Psome was stable enough for longer period (>180 days) of time at 2−8 °C, because LTA along with GC-$SA_{25\%}$ copolymer,[10] increases hydrophobic interaction with drug, which leads to prevention of drug leakage from LTA-L-Psome and no significant changes was found in size and EE.[10] While drug leakage from liposomal ambisome results in decrease in EE and increase in size over a period of time because of its lipid components (Figure 2b). Other two formulations AmB-L-Psome and fungizone were also stable in this condition as reported in our previous publication.[10] Six months storage of LTA-AmB-L-Psome with BSA and plasma did not affect the shape (Figure 3) demonstrates the rigid characteristics of formulation. Further, negligible change in size and PDI of LTA-AmB-L-Psome when incubated with BSA and plasma during 60 min (Supporting Information, Figure S2), also strengthen the rigidness of this delivery system.

The infected J774A and RAW264.7 cell culture study demonstrated a ∼2.5-fold and ∼3.7-fold increase in the overall uptake of LTA-FAmB-L-Psome compared to FAmB-L-Psome (Figure 4(i) and (ii), respectively) create scope to facilitate enhanced drug distribution in macrophage rich liver, spleen, and lung tissues that may be significant for visceral leishmaniasis, as presented in Figure 7. In the case of noninfected macrophages we have observed that uptake of FAmB-L-Psome and LTA-FAmB-L-Psome was similar. This data clearly indicates that LTA-FAmB-L-Psome possess specificity for infected macrophages. This may be attributed to the fact that parasite infected macrophages have over-expression of LTA specific pattern recognition receptors. To further establish this phenomenon we have saturated infected macrophages with lipoteichoic acid before addition of our formulations. In this experiment, it has been observed that when infected macrophage cell lines incubated with lipoteichoic acid, the receptors get saturated with LTA and no free LTA binding sites remain available for uptake of both FAmB-L-Psome (b) and LTA-FAmB-L-Psome (c; Supporting Information, Figure S3(ii)). The overall experiment demonstrates that uptake is mainly driven by LTA specific active targeting. Significantly enhanced uptake of LTA-FAmB-L-Psome compared to FAmB-L-Psome responsible for greater localization of fluorescence inside macrophages, as observed from Figure 5, that supports our results of superior uptake of LTA functionalized L-Psome, where LTA interacts through its two polyanionic hydrophilic acyl chains, become approachable for macrophage pattern recognition receptors such as scavenger receptor together with Toll-like receptors TLR2 and TLR6 and its coreceptors CD14 and CD36.[6,7,22,23]

We compared the tissue distribution and pharmacokinetics of AmB in Wistar rats following IV bolus administration of LTA-AmB-L-Psome, AmB-L-Psome, and commercial formulations. The LTA-AmB-L-Psome, being composed of macrophage targeting ligand LTA decorated on AmB-L-Psome surface, is recognized more rapidly by the mononuclear phagocyte system (MPS such as liver, spleen, lung, etc.), which results in initial rapid clearance from the bloodstream and lower plasma concentration compared to ambisome and AmB-L-Psome, as shown in Table 2. The LTA-AmB-L-Psome rendered AmB to get more concentrated in the macrophage abundant liver and spleen because the delivery system get quickly identified and internalized by macrophages due to presence of LTA bacterial antigen on LTA-AmB-L-Psome surface, while ambisome-treated group showed relatively lesser AmB concentration (Figure 6). Additionally, LTA-AmB-L-Psome showed comparative disposition into lung among AmB-L-Psome and ambisome, and very fewer dispositions in kidney. Indeed, fungizone was reported in multiple studies to be more nephrotoxic than lipid based AmB formulations.[16] The dose-limiting toxicity of AmB results from distribution of the toxic drug to all organs. By involvement of receptor mediated targeting approach using LTA ligand, LTA-AmB-L-Psome will selectively target AmB to the parasite resident macrophages and subsequently released in the lysosomal compartment and in this way eliminate toxicity by preventing drug distribution to kidney. LTA-AmB-L-Psome and AmB-L-Psome showed lower plasma drug concentrations than ambisome, suggests a sustained release rate due to high rigidness and molecular interaction with GC-SA, which may delay AmB release. Pharmacokinetic profile of LTA-AmB-L-Psome, resulting in sustained plasma levels, increased MRT, increased $t_{1/2}$ and decreased clearance compared to fungizone (Table 2). When the AUC of IV administered LTA-AmB-L-Psome is compared with that of ambisome and fungizone (Table 2), the rank order was found to be fungizone < LTA-AmB-L-Psome < AmB-L-Psome < ambisome ($p < 0.05$). This complex kinetics due to LTA biomarker ligand appended with AmB-L-Psome formulation results in reduction of AmB related toxicities and increase in drug efficacy that may be step forward chemotherapeutics using AmB.

The higher phagocytic potentiation by LTA attributed to the fact that, since antigen is the part of cell membrane of Gram-positive bacteria, and after LTA decoration on L-Psome surface, LTA-L-Psome acquire antigen immunostimulatory property of bacteria and quickly get recognized by macrophages in the same manner as in case of bacteria via negative charges and possibly also LTA polyanionic hydrophilic chains. It may thus be concluded that LTA pattern recognition receptor of macrophages (SR, TLR2, TLR6, CD14, CD36) play an important role in phagocytosis by serving as receptors for LTA that form bridges between the macrophages and formulation.[6,7,22,23]

The in vitro and in vivo antileishmanial activity of LTA-AmB-L-Psome was significantly improved compared to other commercial formulations ($p < 0.05$), as shown in Figure 7, since macrophagic targeting potential of LTA decorated L-Psome, advanced new area of targeted drug delivery systems for leishmaniasis chemotherapy. To the best of our knowledge, we are the foremost to explore targeting potential of LTA in L-Psome, a novel drug delivery system. Our data also illustrate that LTA-L-Psome could be a valuable carrier for targeting antileishmanial drugs specifically into parasite resided APC. In view of the fact that LTA decorated L-Psome act as a signal to macrophages for engulfment, get quickly recognized by TLRs and other specific receptors, phagocytosed, and subsequently activate the intracellular signal transduction pathway, which leads to translocation of transcription factor NF-κB into the nucleus through adaptor proteins, such as TIRAP and MyD88, which consecutively activates the pro-inflammatory intracellular signal transduction cascades for expression of cytokine genes.[24,25] The copolymer component GC has been shown to induce pro-inflammatory response through subsequently macrophage activation responsible for rapid parasite killing and digestion.[26,27]

We evaluated several Th-1 (IFN-γ, TNF-α, IL-12) and Th-2 (TGF-β, IL-4 and IL-10) cytokine and chamokines to explore their possible role in *Leishmania*-infected hamsters by treatment with formulations. A protective adaptive immune response

DOI: 10.1021/bm5015156
Biomacromolecules XXXX, XXX, XXX−XXX

against *Leishmania* parasites depends on Th1-tailored milieu with IL-12, TNF-α and IFN-γ cytokines, and inducible nitric oxide synthase (iNOS)-dependent generation of NO, is important for the parasiticidal activity of infected APC.[15] Microbial toxins and cytokines activate APC to kill parasites through expression of iNOS that convert L-arginine to NO effector molecule mediated by L-arginine-NO pathway. The results of present study demonstrated that LTA-functionalized L-Psome induces significantly elevated NO synthesis and iNOS gene expression (Figure 8), which complied with some of the earlier reports.[28−30] Infected control group showed reduced Th-1 cytokine expression in experimental hamsters; while LTA-decorated L-Psome has been shown to induce IFN-γ, IL-12, and TNF-α activities in macrophages, through engagement of LTA ligand with their cognate receptors.[31−33] LTA motif of LTA-AmB-L-Psome act as TLR2 agonist and enhance antigen specific IFN-γ release,[32] while IL-12 release induced through CD14-dependent pathway or by engagement with scavenger receptors.[22,33]

Immunosuppressive Th-2 cell-associated cytokines (TGF-β, IL-10 and IL-4) through their counter-regulatory effect against IL-12 and IFN-γ are responsible for the survival of *Leishmania* parasites in the infected APC[34−38] and enhance the parasite susceptibility by inhibiting NO-mediated killing.[39] Our results demonstrated that LTA functionalized L-Psome treated infected hamsters showed decrease in IL-10 and IL-4 cytokines expression level, subsequently, TGF-β level also decreased, responsible for promotion of IFN-γ and TNF-α level, as shown in Figure 8. Collectively, effective elimination of IL-10, IL-4, and TGF-β synchronizing with the up-regulation of IFN-γ, IL-12, and TNF-α recommend that LTA functionalized L-Psome initiate a strong antileishmanial response involving NO production which potentially accounts for the reduction of parasite burden in the infected hamsters.

The study demonstrated a major reduction in the toxicity of AmB upon incorporation in LTA-L-Psome compared with commercial formulations. We studied in vitro hemolysis, which is a reliable measure for estimating the erythrocyte membrane damage caused in vivo. Figure 9a showed that fungizone has a very high hemolytic effect on Wistar rat erythrocytes, while LTA-decorated AmB-L-Psome has negligible hemolytic potential. Subsequently, LTA-AmB-L-Psome is least toxic to J744A macrophage cell line compared to commercial formulations (Figure 9b). The biochemical analysis revealed that ambisome, a lipid-based formulation showed elevated levels of serum aspartate aminotransferase (ASAT) and alanine aminotransferase (ALAT), the hepatotoxicity markers (Figure 9c), complies with previously reported study,[40] which could be due to the composition and proportion of the lipid associated with AmB. On the contrary, administration of copolymer−lipid based AmB-L-Psome and LTA-AmB-L-Psome in mice did show insignificant increase in the serum ASAT and ALAT levels. Renal toxicity was assessed by estimating serum creatinine, blood urea in treated mice. Though the levels of serum creatinine and blood urea were elevated in mice treated with fungizone, but LTA-AmB-L-Psome, AmB-L-Psome, and ambisome treated mice showed normal levels of creatinine and blood urea giving indication of no renal function alterations (Figure 9c).

This biochemical result defining fungizone and ambisome related toxicities was supported by histopathology of kidney and liver tissues, respectively, as illustrated in Figure 10. Whereas LTA-AmB-L-Psome was found to be nontoxic as observed by normal histopathology of studied tissues. The LTA-AmB-L-Psome was safe and diminished nephrotoxicity even at higher doses due to presence of monomeric form of AmB in formulation.[10,41] Pharmacokinetics and biodistribution of targeted LTA-AmB-L-Psome causes reduction in drug accumulation in kidney tissue and, hence, diminishing nephrotoxicities. Moreover, reduced toxicity observed in case of LTA-AmB-L-Psome are concordant with previous lipid-complexed AmB formulations.[42] Furthermore, it provides evidence that LTA decoration on AmB-L-Psome does not impart any toxicity since it induces cytokines release that might be in the threshold level.

Moreover, excipients and processes used in preparation of LTA-AmB-L-Psome was more economical comparative to lipid based marketed formulations. Furthermore, due to infected macrophage targeting efficiency results in reduction of dose of drug supplementary for reduction in cost.

5. CONCLUSION

LTA-L-Psome can be readily adapted for specific delivery of a variety of chemotherapeutic drugs to APC for intracellular parasitic disease eradication. The prospective advantage of a safe, affordable and efficient therapeutics is predominantly pertinent in low resource nations. Easy architecture of new LTA-AmB-L-Psome delivery system renders scalability features. The receptor-mediated APC targeting and stimulation potential of system and pharmacokinetic distribution results in relevant differences in AmB antileishmanial potential and toxicity. Since, there is a clear relationship between the uptake of AmB and its distribution, immuno-stimulation, efficacy and toxicity. Consequently, LTA-AmB-L-Psome has a better therapeutic index than commercial formulations. Concisely, novel APC targeted LTA-AmB-L-Psome mediated immuno-chemotherapy holds great promise as a safer and effective therapy for intra-APC diseases including VL.

■ ASSOCIATED CONTENT

Supporting Information

Additional experimental details and results of stability (Figure S1), rigidity (Figure S2), and macrophage uptake (Figure S3i,ii) studies. This material is available free of charge via the Internet at http://pubs.acs.org.

■ AUTHOR INFORMATION

Corresponding Author

*Phone:91-522-2771940; 2772450 (4537). Fax: 91-522-2771941.

Notes

The authors declare no competing financial interest.

■ ACKNOWLEDGMENTS

P.K.G. thankfully acknowledges CSIR, New Delhi, India, for awarding fellowship. Authors are thankful to confocal laser scanning microscopy facility at CSIR-National botanical research institute, Lucknow and Electron Microscope Facility at Department of Anatomy, All India Institute of Medical Sciences (AIIMS, New Delhi, India), for providing electron microscope analysis. Financial assistance from CSIR-Network Project BIOCERAM (ESC 0103) is gratefully acknowledged. This is CDRI communication number 8926.

DOI: 10.1021/bm5015156
Biomacromolecules XXXX, XXX, XXX−XXX

REFERENCES

(1) Courret, N.; Frehel, C.; Gouhier, N.; Pouchelet, M.; Prina, E.; Roux, P.; Antoine, J. C. Biogenesis of leishmania-harbouring parasitophorous vacuoles following phagocytosis of the metacyclic promastigote or amastigote stages of the parasites. *J. Cell Sci.* **2002**, *115* (Pt 11), 2303−2316.

(2) McMahon-Pratt, D.; Kima, P. E.; Soong, L. Leishmania amastigote target antigens: the challenge of a stealthy intracellular parasite. *Parasitol Today* **1998**, *14* (1), 31−34.

(3) Wilson, C. B.; Tsai, V.; Remington, J. S. Failure to trigger the oxidative metabolic burst by normal macrophages: possible mechanism for survival of intracellular pathogens. *J. Exp. Med.* **1980**, *151* (2), 328−346.

(4) Asthana, S.; Gupta, P. K.; Chaurasia, M.; Dube, A.; Chourasia, M. K. Polymeric colloidal particulate systems: Intelligent tools for intracellular targeting of antileishmanial cargos. *Exp. Opin. Drug Delivery* **2013**, *10* (12), 1633−1651.

(5) Fischer, W. Physiology of lipoteichoic acids in bacteria. *Adv. Microb. Physiol.* **1988**, *29*, 233−302.

(6) Greenberg, J. W.; Fischer, W.; Joiner, K. A. Influence of lipoteichoic acid structure on recognition by the macrophage scavenger receptor. *Infect. Immun.* **1996**, *64* (8), 3318−3325.

(7) Brown, M. S.; Goldstein, J. L. Lipoprotein metabolism in the macrophage: implications for cholesterol deposition in atherosclerosis. *Annu. Rev. Biochem.* **1983**, *52*, 223−261.

(8) Celis, E. Toll-like receptor ligands energize peptide vaccines through multiple paths. *Cancer Res.* **2007**, *67* (17), 7945−7947.

(9) Ginsburg, I. Role of lipoteichoic acid in infection and inflammation. *Lancet Infect. Dis.* **2002**, *2* (3), 171−179.

(10) Gupta, P. K.; Jaiswal, A. K.; Kumar, V.; Verma, A.; Dwivedi, P.; Dube, A.; Mishra, P. R. Covalent functionalized self-assembled lipo-polymerosome bearing amphotericin B for better management of leishmaniasis and its toxicity evaluation. *Mol. Pharmaceutics* **2014**, *11* (3), 951−963.

(11) Gupta, P. K.; Asthana, S.; Jaiswal, A. K.; Kumar, V.; Verma, A. K.; Shukla, P.; Dwivedi, P.; Dube, A.; Mishra, P. R. Exploitation of lectinized lipo-polymerosome encapsulated amphotericin B to target macrophages for effective chemotherapy of visceral leishmaniasis. *Bioconjugate Chem.* **2014**, *25* (6), 1091−1102.

(12) Morton, R. E.; Evans, T. A. Modification of the bicinchoninic acid protein assay to eliminate lipid interference in determining lipoprotein protein content. *Anal. Biochem.* **1992**, *204* (2), 332−334.

(13) Noble, J. E.; Bailey, M. J. Quantitation of protein. *Methods Enzymol.* **2009**, *463*, 73−95.

(14) Desjardins, P.; Hansen, J. B.; Allen, M. Microvolume protein concentration determination using the NanoDrop 2000c spectrophotometer. *J. Visualized Exp.* **2009**, No. 33, 1610.

(15) Asthana, S.; Jaiswal, A. K.; Gupta, P. K.; Pawar, V. K.; Dube, A.; Chourasia, M. K. Immunoadjuvant chemotherapy of visceral leishmaniasis in hamsters using amphotericin B-encapsulated nano-emulsion template-based chitosan nanocapsules. *Antimicrob. Agents Chemother.* **2013**, *57* (4), 1714−1722.

(16) Boswell, G. W.; Bekersky, I.; Buell, D.; Hiles, R.; Walsh, T. J. Toxicological profile and pharmacokinetics of a unilamellar liposomal vesicle formulation of amphotericin B in rats. *Antimicrob. Agents Chemother.* **1998**, *42* (2), 263−268.

(17) Mookerjee Basu, J.; Mookerjee, A.; Banerjee, R.; Saha, M.; Singh, S.; Naskar, K.; Tripathy, G.; Sinha, P. K.; Pandey, K.; Sundar, S.; Bimal, S.; Das, P. K.; Choudhuri, S. K.; Roy, S. Inhibition of ABC transporters abolishes antimony resistance in leishmania infection. *Antimicrob. Agents Chemother.* **2008**, *52* (3), 1080−1093.

(18) Ding, A. H.; Nathan, C. F.; Stuehr, D. J. Release of reactive nitrogen intermediates and reactive oxygen intermediates from mouse peritoneal macrophages. Comparison of activating cytokines and evidence for independent production. *J. Immunol.* **1988**, *141* (7), 2407−2412.

(19) Murray, H. W.; Nathan, C. F. Macrophage microbicidal mechanisms in vivo: reactive nitrogen versus oxygen intermediates in the killing of intracellular visceral Leishmania donovani. *J. Exp. Med.* **1999**, *189* (4), 741−746.

(20) Davidson, R. N.; di Martino, L.; Gradoni, L.; Giacchino, R.; Gaeta, G. B.; Pempinello, R.; Scotti, S.; Cascio, A.; Castagnola, E.; Maisto, A.; Gramiccia, M.; di Caprio, D.; Wilkinson, R. J.; Bryceson, A. D. Short-course treatment of visceral leishmaniasis with liposomal amphotericin B (AmBisome). *Clin. Infect. Dis.* **1996**, *22* (6), 938−943.

(21) Dietze, R.; Milan, E. P.; Berman, J. D.; Grogl, M.; Falqueto, A.; Feitosa, T. F.; Luz, K. G.; Suassuna, F. A.; Marinho, L. A.; Ksionski, G. Treatment of brazilian kala-azar with a short course of amphocil (amphotericin B cholesterol dispersion). *Clin. Infect. Dis.* **1993**, *17* (6), 981−986.

(22) Dunne, D. W.; Resnick, D.; Greenberg, J.; Krieger, M.; Joiner, K. A. The type I macrophage scavenger receptor binds to gram-positive bacteria and recognizes lipoteichoic acid. *Proc. Natl. Acad. Sci. U.S.A.* **1994**, *91* (5), 1863−1867.

(23) Lebeer, S.; Vanderleyden, J.; De Keersmaecker, S. C. Host interactions of probiotic bacterial surface molecules: comparison with commensals and pathogens. *Nat. Rev. Microbiol* **2010**, *8* (3), 171−184.

(24) Hasty, D. L.; Meron-Sudai, S.; Cox, K. H.; Nagorna, T.; Ruiz-Bustos, E.; Losi, E.; Courtney, H. S.; Mahrous, E. A.; Lee, R.; Ofek, I. Monocyte and macrophage activation by lipoteichoic acid is independent of alanine and is potentiated by hemoglobin. *J. Immunol.* **2006**, *176* (9), 5567−5576.

(25) Takeda, K.; Akira, S. Toll-like receptors in innate immunity. *Int. Immunol.* **2005**, *17* (1), 1−14.

(26) Bajaj, G.; Van Alstine, W. G.; Yeo, Y. Zwitterionic chitosan derivative, a new biocompatible pharmaceutical excipient, prevents endotoxin-mediated cytokine release. *PLoS One* **2012**, *7* (1), e30899.

(27) Oster, C. N.; Nacy, C. A. Macrophage activation to kill Leishmania tropica: kinetics of macrophage response to lymphokines that induce antimicrobial activities against amastigotes. *J. Immunol.* **1984**, *132* (3), 1494−1500.

(28) Hattor, Y.; Kasai, K.; Akimoto, K.; Thiemermann, C. Induction of NO synthesis by lipoteichoic acid from Staphylococcus aureus in J774 macrophages: involvement of a CD14-dependent pathway. *Biochem. Biophys. Res. Commun.* **1997**, *233* (2), 375−379.

(29) Kuo, C. T.; Chiang, L. L.; Lee, C. N.; Yu, M. C.; Bai, K. J.; Lee, H. M.; Lee, W. S.; Sheu, J. R.; Lin, C. H. Induction of nitric oxide synthase in RAW 264.7 macrophages by lipoteichoic acid from Staphylococcus aureus: involvement of protein kinase C- and nuclear factor-kB-dependent mechanisms. *J. Biomed. Sci.* **2003**, *10* (1), 136−145.

(30) Chang, Y. C.; Li, P. C.; Chen, B. C.; Chang, M. S.; Wang, J. L.; Chiu, W. T.; Lin, C. H. Lipoteichoic acid-induced nitric oxide synthase expression in RAW 264.7 macrophages is mediated by cyclooxygenase-2, prostaglandin E2, protein kinase A, p38 MAPK, and nuclear factor-kappaB pathways. *Cell. Signalling* **2006**, *18* (8), 1235−1243.

(31) Matsuguchi, T.; Takagi, A.; Matsuzaki, T.; Nagaoka, M.; Ishikawa, K.; Yokokura, T.; Yoshikai, Y. Lipoteichoic acids from Lactobacillus strains elicit strong tumor necrosis factor alpha-inducing activities in macrophages through Toll-like receptor 2. *Clin. Diagn. Lab. Immunol.* **2003**, *10* (2), 259−266.

(32) Dammermann, W.; Wollenberg, L.; Bentzien, F.; Lohse, A.; Luth, S. Toll like receptor 2 agonists lipoteichoic acid and peptidoglycan are able to enhance antigen specific IFNgamma release in whole blood during recall antigen responses. *J. Immunol. Methods* **2013**, *396* (1−2), 107−115.

(33) Cleveland, M. G.; Gorham, J. D.; Murphy, T. L.; Tuomanen, E.; Murphy, K. M. Lipoteichoic acid preparations of gram-positive bacteria induce interleukin-12 through a CD14-dependent pathway. *Infect. Immun.* **1996**, *64* (6), 1906−1912.

(34) Gantt, K. R.; Schultz-Cherry, S.; Rodriguez, N.; Jeronimo, S. M.; Nascimento, E. T.; Goldman, T. L.; Recker, T. J.; Miller, M. A.; Wilson, M. E. Activation of TGF-beta by Leishmania chagasi: Importance for parasite survival in macrophages. *J. Immunol.* **2003**, *170* (5), 2613−2620.

(35) Barral-Netto, M.; Barral, A.; Brownell, C. E.; Skeiky, Y. A.; Ellingsworth, L. R.; Twardzik, D. R.; Reed, S. G. Transforming growth

DOI: 10.1021/bm5015156
Biomacromolecules XXXX, XXX, XXX−XXX

factor-beta in leishmanial infection: a parasite escape mechanism. *Science* **1992**, *257* (5069), 545−548.
(36) Holaday, B. J.; Pompeu, M. M.; Jeronimo, S.; Texeira, M. J.; Sousa Ade, A.; Vasconcelos, A. W.; Pearson, R. D.; Abrams, J. S.; Locksley, R. M. Potential role for interleukin-10 in the immunosuppression associated with kala azar. *J. Clin. Invest.* **1993**, *92* (6), 2626−2632.
(37) Karp, C. L.; el-Safi, S. H.; Wynn, T. A.; Satti, M. M.; Kordofani, A. M.; Hashim, F. A.; Hag-Ali, M.; Neva, F. A.; Nutman, T. B.; Sacks, D. L. In vivo cytokine profiles in patients with kala-azar. Marked elevation of both interleukin-10 and interferon-gamma. *J. Clin. Invest.* **1993**, *91* (4), 1644−1648.
(38) Asthana, S.; Jaiswal, A. K.; Gupta, P. K.; Dube, A.; Chourasia, M. K. Th-1 biased immunomodulation and synergistic antileishmanial activity of stable cationic lipid-polymer hybrid nanoparticle: Biodistribution and toxicity assessment of encapsulated amphotericin B. *Eur. J. Pharm. Biopharm.* **2014**, *89*, 62−73.
(39) Vouldoukis, I.; Becherel, P. A.; Riveros-Moreno, V.; Arock, M.; da Silva, O.; Debre, P.; Mazier, D.; Mossalayi, M. D. Interleukin-10 and interleukin-4 inhibit intracellular killing of Leishmania infantum and Leishmania major by human macrophages by decreasing nitric oxide generation. *Eur. J. Immunol.* **1997**, *27* (4), 860−865.
(40) Larabi, M.; Pages, N.; Pons, F.; Appel, M.; Gulik, A.; Schlatter, J.; Bouvet, S.; Barratt, G. Study of the toxicity of a new lipid complex formulation of amphotericin B. *J. Antimicrob. Chemother.* **2004**, *53* (1), 81−88.
(41) Gupta, P. K.; Jaiswal, A. K.; Asthana, S.; Verma, A.; Kumar, V.; Shukla, P.; Dwivedi, P.; Dube, A.; Mishra, P. R. Self assembled ionically sodium alginate cross-linked amphotericin B encapsulated glycol chitosan stearate nanoparticles: Applicability in better chemotherapy and non-toxic delivery in visceral leishmaniasis. *Pharm. Res.* **2014**, DOI: 10.1007/s11095-014-1571-4.
(42) Yardley, V.; Croft, S. L. A comparison of the activities of three amphotericin B lipid formulations against experimental visceral and cutaneous leishmaniasis. *Int. J. Antimicrob. Agents* **2000**, *13* (4), 243−248.

DOI: 10.1021/bm5015156
Biomacromolecules XXXX, XXX, XXX−XXX